

## Rapid Communications

The *Rapid Communications* section is intended for the accelerated publication of important new results. Manuscripts submitted to this section are given priority in handling in the editorial office and in production. A *Rapid Communication* may be no longer than 3½ printed pages and must be accompanied by an abstract. Page proofs are sent to authors, but, because of the rapid publication schedule, publication is not delayed for receipt of corrections unless requested by the author.

### Shape effects in $h_{11/2}$ and $g_{7/2}$ bands in $^{159}\text{Tm}$

A. J. Larabee, L. H. Courtney, S. Frauendorf,\* and L. L. Riedinger

*Department of Physics and Astronomy, The University of Tennessee,  
Knoxville, Tennessee 37996-1200*

J. C. Waddington

*McMaster University, Hamilton, Ontario, L8S 4M1 Canada*

M. P. Fewell,† N. R. Johnson, I. Y. Lee, and F. K. McGowan

*Oak Ridge National Laboratory, Oak Ridge, Tennessee 37830*

(Received 27 February 1984)

The  $\frac{7}{2}[523]$  and  $\frac{7}{2}[404]$  bands are observed in  $^{159}\text{Tm}$  to  $I = \frac{61}{2}$  and  $\frac{43}{2}$ , respectively, well beyond the  $i_{13/2}$  neutron backbend. Before the backbend, the  $\frac{7}{2}[523]$  band exhibits large signature splitting, the  $\frac{7}{2}[404]$  none, which is interpreted as resulting from the very different driving influences of the  $K = \frac{7}{2}$ ,  $h_{11/2}$ , and  $g_{7/2}$  orbits, respectively, on the core triaxiality. The  $i_{13/2}$  neutron alignment changes the signature splitting in each band as a result of its dominant driving force to positive values of  $\gamma$ . Measured  $B(M1; I \rightarrow I-1)/B(E2; I \rightarrow I-2)$  values increase dramatically after the backbend, and this is explained in terms of calculated increases in the  $M1$  transition rates and decreases in the  $E2$  rates.

The triaxial  $N = 90$  nuclei are generally viewed as rather soft with shapes that may be profoundly affected by rotation and by quasiparticle alignment. One approach to determine the nuclear shape is to study the energy splitting between the two signatures of medium-to-high  $K$  bands, since recent calculations<sup>1,2</sup> have shown this to be rather sensitive to the size of  $\gamma$ , the core triaxiality parameter. We present here the best example to data of the very different polarizing influences on the soft  $N = 90$  core by two different quasiparticle excitations in  $^{159}\text{Tm}$ .

Two  $K = \frac{7}{2}$  bands are observed, based on the  $h_{11/2}$  and  $g_{7/2}$  quasiproton orbitals. These two bands have very different degrees of signature splitting (i.e., the energy difference between the favored and unfavored components of the band), which are explained here as the effect of the  $h_{11/2}$  and  $g_{7/2}$  orbitals having distinctly different values of  $\gamma$ . In addition,  $B(M1)/B(E2)$  ratios are measured in both bands and found to reflect the differences in signature splittings. Furthermore, the  $B(M1)/B(E2)$  values increase dramatically after the backbend in each band and the classical vector model of Ref. 3 is used to explain this as an effect of enhanced  $M1$  and decreased  $E2$  matrix elements.

The level scheme for  $^{159}\text{Tm}$  (Fig. 1) has been constructed from experiments involving the  $^{148}\text{Sm}(^{14}\text{N}, 3n)$  reaction at the McMaster University tandem accelerator<sup>4</sup> and the  $^{141}\text{Pr}(^{22}\text{Ne}, 4n)$  reaction at the Oak Ridge Isochronous Cyclotron. In the Oak Ridge measurement, two large NaI counters were used as a total energy filter and 7 Ge detectors counted the primary  $\gamma$ - $\gamma$  coincidence data. Triple coin-

cidences between the Ge detectors were accumulated and subsequently analyzed to give approximately 240 million  $\gamma$ - $\gamma$  pairs in coincidence with the total energy range which emphasized the  $^{159}\text{Tm}$  reaction product. Angular distribution data and angular correlation data were analyzed to assign spins and extract multiple mixing ratios.

Two distinct rotational structures, composed of stretched  $E2$  and crossover  $E2/M1$  transitions, were assigned based upon the coincidence and angular distribution data. The structure on the left in Fig. 1 is yrast based upon the larger population intensity, and has been assigned previously<sup>4,5</sup> as a band built upon the  $\frac{7}{2}[523]$  Nilsson configuration. The spins and parities of the other band in Fig. 1 are determined largely by the stretched dipole nature of the 717.5 and 790.8 keV transitions feeding the  $\frac{21}{2}^-$  and  $\frac{23}{2}^-$  levels, respectively, of the  $\frac{7}{2}^- [523]$  band. A further argument against negative parity for the band on the right is that the two  $I = \frac{7}{2}$  bandheads would have negative parity and be split by only 36 keV with little apparent mixing. This band is evidently built upon the  $\frac{7}{2}[404]$  Nilsson orbital. Possible low energy transitions from the backbends to an  $I = \frac{5}{2}$  ground state<sup>6</sup> have not been observed. Parts of this level scheme have been reported previously.<sup>7</sup>

Sharp backbends occur in both the  $h_{11/2}$  and  $g_{7/2}$  structures, where the  $i_{13/2}$  neutron alignment results in the crossing of the one-quasiparticle bands by three-quasiparticle bands of greater alignment. Below the backbend, in the  $h_{11/2}$  band ( $I < \frac{29}{2}$ ), a large energy difference between the

two signatures is clearly present. The unfavored band ( $I = \frac{13}{2}, \frac{17}{2}, \dots$ , i.e.,  $\alpha = +\frac{1}{2}$  in the notation of Refs. 1-3 and 8) lies at least 100 keV above the favored structure ( $\alpha = -\frac{1}{2}$ ). After the backbend ( $I > \frac{37}{2}$ ), the energy difference between the two signatures is less than 10 keV. In contrast, the  $g_{7/2}$  band shows essentially no splitting before or after the backbend. The very different degree of signature splitting in these two  $K = \frac{7}{2}$  bands below the back-

bend is rather remarkable and likely indicates that the nucleus has different shapes in these two modes.

The observed behavior of the  $K = \frac{7}{2}$  bands in  $^{159}\text{Tm}$  is consistent with the predicted<sup>1,2</sup> influence of these quasiparticle orbits on the degree of the core triaxiality  $\gamma$ . In the case of the  $\frac{7}{2}^- [523]$  band, the chemical potential  $\lambda$ , for protons is in the middle of the  $h_{11/2}$  shell. Calculations using the cranked shell model (CSM) show that for this value of  $\lambda$ , the  $\alpha = -\frac{1}{2}$  signature of the  $\frac{7}{2}^- [523]$  quasiparticle state has a well-defined minimum at  $\omega = 0.3 \text{ MeV}/\hbar$  and  $\gamma \approx -50^\circ$  while the  $\alpha = +\frac{1}{2}$  signature is less  $\gamma$  driving with a fairly shallow minimum at  $\gamma \approx -70^\circ$ ; this produces a rather large splitting. The observation of a large signature splitting indicates that the nucleus does indeed follow the driving influence of the  $h_{11/2}$  orbital. Adding the  $\gamma$  dependence of these quasiparticle orbits to the expected hydrodynamical behavior of the core ( $V_{p0} \cos 3\gamma$ )<sup>1</sup> gives equilibrium values of  $\gamma \approx -25^\circ$  ( $\alpha = -\frac{1}{2}$ ) and  $\gamma \approx -14^\circ$  ( $\alpha = +\frac{1}{2}$ ) at  $\omega = 0.3 \text{ MeV}/\hbar$ . The value of  $V_{p0} = -0.89 \text{ MeV}$  is chosen to reproduce the signature splitting seen in the  $\frac{7}{2}^- [523]$  band.

After the backbend, two  $i_{13/2}$  quasineutrons are added. At  $N \sim 90$  the  $\lambda$  for neutrons is at the beginning of the  $i_{13/2}$  shell, which leads to an orbit driving the core towards small positive  $\gamma$ , where the signature splitting in the  $h_{11/2}$  band disappears. The neutrons have a stronger driving force than

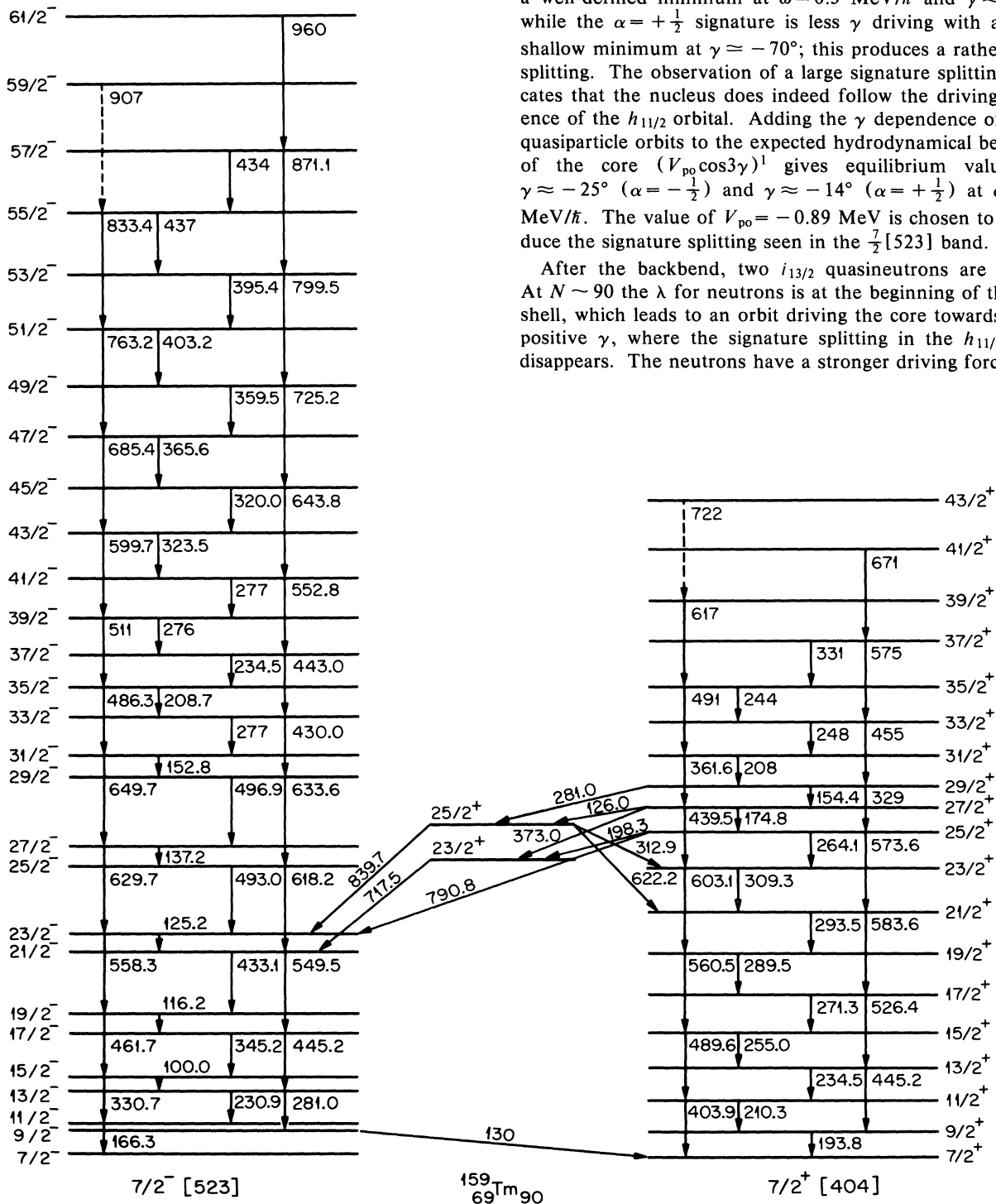


FIG. 1. Level scheme for  $^{159}\text{Tm}$ .

the protons and thus the combined influence of these three quasiparticles on the core yields equilibrium values of  $\gamma \sim 0^\circ$  for both signatures, which is consistent with the observed disappearance of the signature splitting. This  $\gamma$  flip-flop has already been observed in  $^{155}\text{Ho}$  (Ref. 9) and  $^{81}\text{Kr}$  (Ref. 10) and has been discussed in detail in the former case in Ref. 1.

In the case of the  $\frac{7}{2}[404]$  band, the  $\lambda$  for protons is at the top of the  $g_{7/2}$  shell. Such orbits, with  $j$  along the symmetry axis, do not drive the core to triaxial shapes. In the CSM calculations, the quasiparticle energy is constant for  $-30^\circ < \gamma < 30^\circ$  and the equilibrium shape simply corresponds to the hydrodynamical shape of the core,  $\gamma \sim -90^\circ$  at  $\omega = 0.23 \text{ MeV}/\hbar$ . The two  $i_{13/2}$  particles again provide the dominant driving force in the three-quasiparticle band and  $\gamma \sim 0^\circ$  results. The CSM calculations predict no signature splitting in this region of the calculated  $\gamma$  deformation and indeed no splitting is observed immediately before or after the backbend in this band.

The transition matrix elements within these bands can be used to test this interpretation of the observed signature splittings. Branching and mixing ratios for many of the transitions in both bands have been extracted, which can give a detailed comparison of  $M1/E2$  ratios of matrix elements before and after the backbends. The  $B(M1; I \rightarrow I-1)/B(E2; I \rightarrow I-2)$  values for many of the states in the  $h_{11/2}$  and  $g_{7/2}$  bands are extracted from measured branching ratios and displayed in Fig. 2. Hagemann *et al.*<sup>11</sup> have reported an enhancement of this  $B(M1)/B(E2)$  ratio in the crossing region of the backbend in  $^{157}\text{Ho}$ , but here we emphasize extraction of ratios for states not involved in the backbend in order to probe the quasiparticle influence in

well-aligned bands. The observed increase in the  $M1/E2$  ratio in  $^{159}\text{Tm}$  is quite dramatic and consistent in the two observed bands. Measured mixing ratios of the  $I \rightarrow I-1$  transitions in the  $h_{11/2}$  band also show an  $M1/E2$  enhancement after the backbend, averaging  $\delta = 0.30 \pm 0.07$  before the backbend and  $0.03 \pm 0.03$  after.

Classically,  $M1$  radiation is generated by the time-dependent (perpendicular) component of magnetic vector as it precesses about the rotation axis. In a cranking approach, it is assumed that the rotational axis is perpendicular to the symmetry axis ( $I_z$ ) and thus the alignment of  $i_{13/2}$  neutrons along this rotation axis ( $I_x$ ) would not obviously influence the  $M1$  rates between the two signatures of the  $h_{11/2}$  or  $g_{7/2}$  bands.<sup>12</sup> However, the recent approach of Dönau and Frauendorf<sup>3</sup> takes account of the fact that the total angular momentum  $I$  is the rotational axis of the system, and is different from  $I_x$  for high- $K$  bands. The angular momentum along  $I_x$ , coming from the aligned  $i_{13/2}$  neutrons, can then be resolved into a component along the  $I$  axis and a component perpendicular. The perpendicular component can contribute to the  $M1$  transition probabilities.

Using such a geometrical approach, Dönau and Frauendorf<sup>3</sup> show that particles aligning during the backbending process are able to contribute coherently to the time-dependent component of the magnetic vector. If the  $g$  factor ( $g_1 - g_R$ ) for the one-quasiparticle state below the backbend (with aligned angular momentum  $i_1$ ) and the  $g$  factor ( $g_2 - g_R$ ) for the two quasiparticles aligning at the backbend (with  $i_2$ ) have opposite signs, then the time-dependent component of the magnetic moment is increased, giving rise to an enhancement of the  $M1$  rate. This can clearly be seen in the expression for the  $B(M1)/B(E2)$  ratio

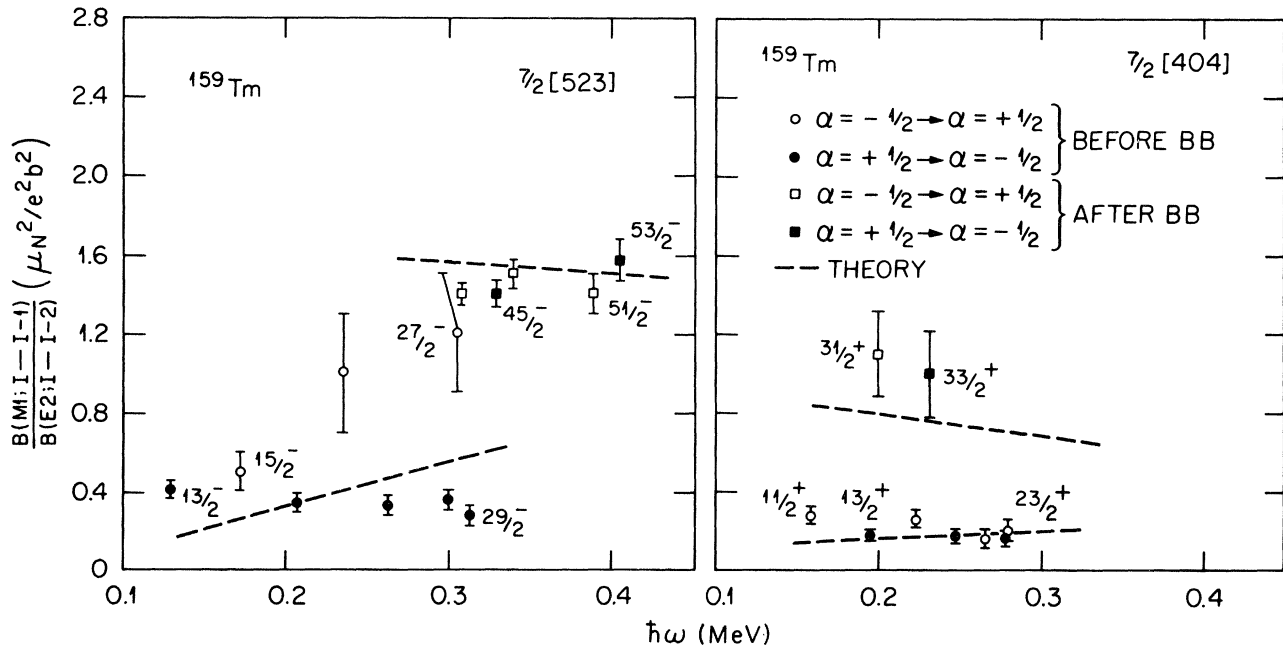


FIG. 2. Ratio of the stretched  $M1$  to stretched  $E2$  reduced transition probabilities for members of the  $\frac{7}{2}[523]$  band (left) and the  $\frac{7}{2}[404]$  band (right) in  $^{159}\text{Tm}$ . Experimental values come from observed branching ratios, the theoretical values from Dönau and Frauendorf (Ref. 3). Theoretical parameters used were: ( $g_1 - g_R$ ) = 0.92,  $i_1 = 4\hbar$  ( $h_{11/2}$  protons); ( $g_1 - g_R$ ) = 0.42,  $i_1 = 2\hbar$ ,  $\gamma = -9^\circ$  ( $g_{7/2}$  protons); ( $g_2 - g_R$ ) = -0.52,  $i_2 = 9.5\hbar$ ,  $\gamma = 0^\circ$  ( $i_{13/2}$  neutrons); and  $Q_0 = 5 \text{ eb}$ . For the  $\frac{7}{2}[523]$  band, signature-averaged values were used below the backbend, where  $\gamma = -25^\circ$  ( $\alpha = -\frac{1}{2}$ ) and  $\gamma = -14^\circ$  ( $\alpha = +\frac{1}{2}$ ).

$$\frac{B(M1; I \rightarrow I-1)}{B(E2; I \rightarrow I-2)} = \frac{12}{5Q_0^2 \cos^2(30^\circ + \gamma)} \left( 1 - \frac{K^2}{(I - \frac{1}{2})^2} \right)^{-2} \frac{K^2}{I^2} \{ (g_1 - g_R) [(I^2 - K^2)^{1/2} - i_1] - (g_2 - g_R) i_2 \}^2. \quad (1)$$

This expression has been modified from that of Ref. 3 to include the effect on the  $E2$  rate of the nonzero  $\gamma$ .

A substantial increase in the  $B(M1)/B(E2)$  ratio is evident in Fig. 2. In the theory, this results not only from an increase of the  $B(M1)$  rate arising from the  $g$  factor of the two aligned  $i_{13/2}$  neutrons but also from a decrease in the  $B(E2)$  due to the loss in collectivity as the  $\gamma$  shifts from negative values to near  $0^\circ$ . Recent Hartree-Fock-Bogoluibov calculations by the Lund group<sup>13</sup> indicate that only a small decrease ( $< 10\%$ ) in  $\epsilon_2$  is expected after the backbend, which affects the calculated ratios only slightly. The calculations presented here have assumed a constant  $\epsilon_2$  deformation throughout the structure.

The results of the calculation based on Eq. (1) are illustrated by the dashed lines in Fig. 2. The  $\gamma$  values used are those extracted from a fit to the observed signature splittings in the bands, as described above. There is a qualitative agreement with the experimental values for the  $\frac{7}{2}[404]$  band and above the backbend in the  $\frac{7}{2}[523]$  band. However, below the backbend in the latter the experimental points are enhanced for the  $\alpha = -\frac{1}{2}$  to  $+\frac{1}{2}$  transitions and depressed for the  $\alpha = \frac{1}{2}$  to  $-\frac{1}{2}$  transitions. This effect was explained in Ref. 3 as resulting from a  $(1 \pm \Delta e'/\hbar\omega)^2$  factor in Eq. (1), which depends on the energy of the signature splitting. Since we have postulated that the signature splitting in the  $h_{11/2}$  band results both from a transition to the rotation-aligned coupling scheme and from different  $\gamma$  deformations for the two signatures, this expression has not been used. The increase in the  $B(M1)/B(E2)$  ratio after the backbend predicted by the theory for the  $\frac{7}{2}[523]$  band is in fairly good quantitative agreement with the experimentally observed increase, if at a given frequency the signature averaged experimental ratio below the backbend is compared with the experimental ratio above. For the  $\frac{7}{2}[404]$  band the theoretical increase in the ratio after the backbend falls somewhat short of the observed increase. However, the general qualitative agreement strengthens the conclusions concerning the shape change.

In conclusion, a change in the signature splitting in the

energies and in the  $B(M1; I \rightarrow I-1)/B(E2; I \rightarrow I-2)$  values is observed in the  $h_{11/2}$  proton band through the neutron backbend, and this change is attributed to the differing driving influences of these quasiparticles to triaxial shapes. In the  $g_{7/2}$  proton band no splitting is observed before or after the backbend since that orbit always has an axial shape. Equilibrium  $\gamma$  values are extracted by comparison of the energy splittings to the cranked shell model. In addition, a large increase in  $B(M1; I \rightarrow I-1)/B(E2; I \rightarrow I-2)$  values are observed in both bands after the backbend. These increases are explained as a result of both a decrease in the  $E2$  transition rates after the backbend ( $\gamma$  becomes positive) and an increase in the  $M1$  rates (the  $g_K - g_R$  of the aligned  $i_{13/2}$  neutrons contributes). These observations thus demonstrate in some detail the differing influences of various quasiparticle orbits in the rather soft  $N = 90$  shapes. There are separate measurements of the changes in the  $E2$  and in the  $M1$  transition rates due to the alignment of quasiparticles in a backbend. In  $^{160}\text{Yb}$ , Fewell *et al.*<sup>14</sup> have observed a decrease in  $B(E2)$  values after the backbend, suggesting a movement to positive values of  $\gamma$  as discussed here. In  $^{81}\text{Kr}$ , Funke *et al.*<sup>10</sup> directly measured an increase in  $B(M1)$  values after the  $g_{9/2}$  proton backbend, and explained it using the model of Ref. 3. Both effects are needed to explain the observed  $B(M1)/B(E2)$  changes induced by the  $i_{13/2}$  neutron backbend in  $^{159}\text{Tm}$ . An important future measurement would be a lifetime experiment on  $^{159}\text{Tm}$ , in order to directly extract the  $B(E2)$  values before and after the backbend. This would bring even more understanding to quasiparticle-dependent shape effects in the  $N = 90$  transition region.

The authors wish to express our appreciation to G. Leander for his comments and participation in discussions. Research at the University of Tennessee is supported by the U.S. Department of Energy under Contract No. DE-AS05-76ER0-4936. At Oak Ridge National Laboratory, the work is supported by the Department of Energy under Contract No. W-7405-eng-26 with the Union Carbide Corporation.

\*Permanent address: Central Institute for Nuclear Research, Rosendorf 8051, Dresden PB 19, German Democratic Republic.

<sup>†</sup>Present address: Department of Nuclear Physics, Australian National University, Canberra, Australian Capitol Territory 2601, Australia.

<sup>1</sup>S. Frauendorf and F. R. May, Phys. Lett. **128B**, 245 (1983).

<sup>2</sup>G. A. Leander, S. Frauendorf, and F. R. May, in *Proceedings of the Conference on High Angular Momentum Properties of Nuclei, Oak Ridge, 1982*, edited by N. R. Johnson (Harwood Academic, New York, 1983), p. 281.

<sup>3</sup>F. Dönau and S. Frauendorf, Ref. 2, p. 143.

<sup>4</sup>A. J. Larabee and J. C. Waddington, Phys. Rev. C **24**, 2367 (1981).

<sup>5</sup>R. Holzmann, J. Kuzminski, M. Loiselet, M. A. Van Hove, and J. Vervier, Ref. 2, Vol. 1; Phys. Rev. Lett. **50**, 1834 (1983).

<sup>6</sup>C. Ekstrom, M. Olsmats, and B. Wannberg, Nucl. Phys. **A170**, 649 (1971).

<sup>7</sup>L. L. Riedinger, L. H. Courtney, A. J. Larabee, J. C. Waddington, M. P. Fewell, N. R. Johnson, I. Y. Lee, and F. K. McGowan,

Ref. 2, Vol. 1.

<sup>8</sup>R. Bengtsson and S. Frauendorf, Nucl. Phys. **A327**, 139 (1979).

<sup>9</sup>M. D. Devous and T. T. Sugihara, Z. Phys. A **288**, 79 (1978); C. Foin, S. Andre, D. Barneoud, J. Boutet, G. Bastin, M. G. Desthuilliers, and J. P. Thibaud, Nucl. Phys. **A324**, 182 (1979).

<sup>10</sup>L. Funke, F. Dönau, J. Döring, P. Kemnitz, E. Will, G. Winter, L. Hildingsson, A. Johnson, and Th. Lindblad, Phys. Lett. **120B**, 301 (1983).

<sup>11</sup>G. B. Hagemann, J. D. Garrett, B. Herskind, G. Sletten, P. O. Tjom, A. Henriques, F. Ingebretsen, J. Rekstad, G. Lovhoiden, and T. F. Thorsteinsen, Phys. Rev. C **25**, 3224 (1982).

<sup>12</sup>I. Hamamoto, Phys. Lett. **102B**, 225 (1981); **106B**, 281 (1981).

<sup>13</sup>R. Bengtsson, Y. S. Chen, J. Y. Zhang, and S. Åberg, Nucl. Phys. **A405**, 221 (1983).

<sup>14</sup>M. P. Fewell, C. Baktash, M. W. Guidry, J. S. Hattula, N. R. Johnson, I. Y. Lee, F. K. McGowan, H. Ower, S. C. Pancholi, L. L. Riedinger, and J. C. Wells, Ref. 2, p. 69.